Analytical modeling of organic solar cells and photodiodes

S. Altazin,[1,2] R. Clerc,[2,a)] R. Gwoziecki,[1] G. Pananakakis,[2] G. Ghibaudo,[2] and C. Serbutoviez[1]
[1]*Printed Device Lab, LITEN, CEA, Grenoble, France*
[2]*IMEP—LAHC, Minatec, Grenoble, France*

An analytical and physically based expression of organic solar cell I-V characteristic under dark and illuminated conditions has been derived. This model has been found in very good agreement with both experimental data and drift-diffusion numerical simulations accounting for the coupling with Poisson equation and optical propagation. © *2011 American Institute of Physics.* [doi:10.1063/1.3643126]

The feasibility of solar cells by low cost processing on large and flexible surfaces have made organic photovoltaic technologies more and more attractive.[1–3] Similarly, interest is also growing for large area light sensors based on matrix of organic photodiodes.[2,3]

The physics and modeling of such photo sensitive devices have been extensively investigated in the literature.[4–9] However, this has been achieved mostly by means of numerical solutions of drift-diffusion transport equations, coupled with Poisson equation, accounting for electron-hole pair dissociation and light propagation. Most of the previous analytical models,[10,11] derived for compact model application, are based on empirical arguments deduced by analogy with classical silicon PN junction models. In Ref. 12, a more physically based model of the illuminated current has been proposed, taking into account the mechanism of electron-hole pair dissociation. However, in this work, the drift and diffusion transport of charges has been ignored, making impossible to reproduce both dark currents and illuminated characteristics around the open circuit voltage V_{OC}. Also, the propagation of light through the device has not been considered.

The aim of this work is thus to derive a physically based analytical model including in the same approach dark and illuminated currents, the drift-diffusion transport of carriers, the electron-hole pair dissociation and optical propagation. In a first step, such closed form expressions are derived in the case of a constant generation rate of bounded electron-hole pairs within the device. These results are generalized, in a second step, to the case of a nonconstant generation rate, using optical simulations. Comparisons have been made with both numerical simulations and experimental data taken from the literature.

As in previous publications,[4–9] the approach used in this work relies on the following approximations. First of all, transport of charges has been assumed to follow the 1D drift-diffusion equations. Then, the mixture of two semiconductor materials (one donor, typically a polymer derived from p-phenylenevinylene (PPV) (Refs. 6 and 7) or poly 3-hexylthiophene (P3HT) (Refs. 8, 9 and 11) and one acceptor, typically a nano-structured fullerene material such as [6, 6]-phenyl C61 butyric acid methyl ester (PCBM)

(Refs. 6–12)) composing the active layer of the device has been modeled by a single meta-material, having the Homo of the donor material and the Lumo of the acceptor semiconductor. In this approach, the interpenetration of donor and acceptor material is supposed to be much smaller than the exciton diffusion length, ignoring the impact of a nonhomogenous phase separation. Moreover, the photogeneration of free charge carriers has been taken into account by the geminate recombination theory of Onsager[13,14] and Braun.[15] In addition, as in most previous studies, only the geminate bimolecular recombination[16] mechanism has been taken into account, neglecting in particular the contribution of traps, which have been found to play a role mostly in dark conditions, and in some specific materials.[17] Metallic contacts have been assumed almost Ohmic and described by applying the standard "fixed electron and hole concentration" boundary conditions.[18] Finally, in the numerical approach, the Poisson equation is solved self-consistently with the continuity equation.

The main approximation leading to a closed form solution consists in assuming the electric field uniform as in Ref. 11, which is generally the case in thin active layer, featuring electron and hole with similar mobilities. This point will be discussed in more details later on. Under this approximation, the electrostatic field is simply given by

$$E = \frac{V_a + \Delta\Phi_2 - \Delta\Phi_1}{L}, \quad (1)$$

where L is the active layer thickness, $\Delta\Phi_1$ (respectively, $\Delta\Phi_2$) the work-function difference between the left (respectively, right) electrode and the semiconductor, and V_a the applied bias between $x = 0$ and $x = L$.

Following Koster and co workers in Ref. 6, using the drift and diffusion formalism, the continuity equation can be written as

$$-\frac{k_b T}{e}\mu_p \frac{d^2 p}{dx^2} + E\mu_p \frac{dp}{dx} = P(E)G - (1 - P(E))R, \quad (2)$$

where G is the generation rate of bounded electron-hole pairs, P(E) the probability for an exciton to be dissociated into free charges, calculated according to the Onsager Braun theories.[14,15] The bimolecular (or Langevin's) recombination rate R is given by[16]

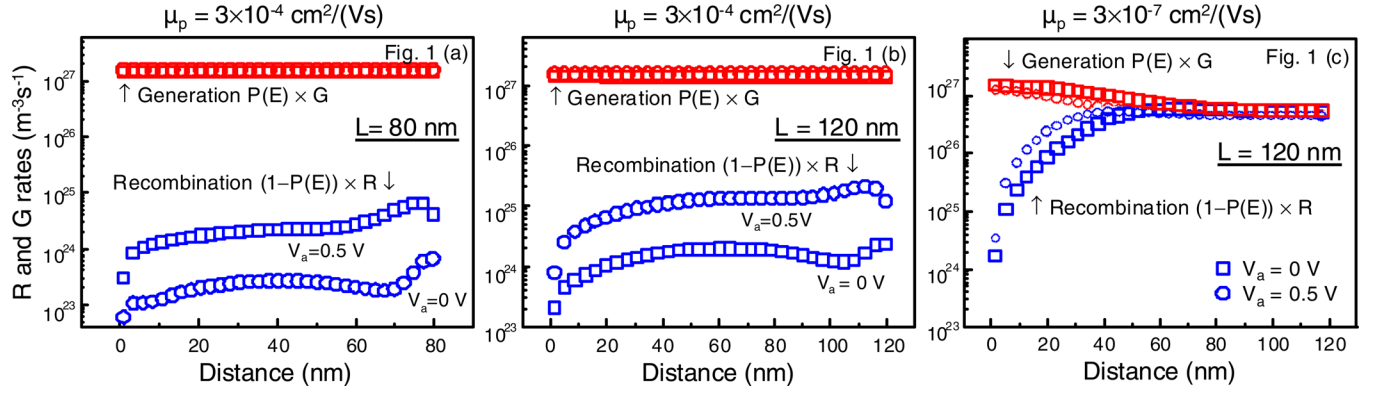a)Author to whom correspondence should be addressed. Electronic mail: clerc@enserg.fr.

FIG. 1. (Color online) Comparison of the relative amplitude of the generation term $P(E) \times G$ and the recombination term $(1-P(E)) \times R$, for two active layer thicknesses: $L = 80$ nm (a) and $L = 120$ nm (b). Bias are $V_a = 0$ V and $V_a = 0.5$ V. In (a) and (b), parameters for these simulations have been taken from Ref. 6: $\Delta\Phi_1 = 0.46$ eV, $\Delta\Phi_2 = -0.46$ eV, $\mu_p = 3 \times 10^{-4}$ cm^2 V^{-1} s^{-1}, $\mu_n = 2.5 \times 10^{-3}$ cm^2 V^{-1}, $G = 1.8 \times 10^{27}$ m^{-3} s^{-1}, $k_f = 1.2 \times 10^6$ s^{-1}, $E_b = 0.326$ eV, $V_a = 0$ V, $\varepsilon_r = 3$. In (c), parameters are the same, except the hole mobility $\mu_p = 3 \times 10^{-7}$ cm^2 V^{-1} s^{-1}.

$$R = e \frac{\mu_p + \mu_n}{2\varepsilon} (np - n_i^2), \qquad (3)$$

where ε represents the dielectric constant and n_i the intrinsic carrier density of electrons and holes.

As illustrated in Figs. 1(a) and 1(b), numerical resolution of coupled Poisson and drift-diffusion equations have shown that the recombination term $(1-P) \times R$ in Eq. (2) can be neglected in front of the generation term $P \times G$. This approximation requires the following explanations.

First of all, as illustrated in Fig. 1(c), it has to be noticed that this approximation is no longer valid when electrons and holes have very different mobility values, i.e., according to our simulations, differing from more than a factor ~50. In this latter case, because of the large difference in transport properties between electrons and holes, a charge tend to accumulate inside the active layer. In this case, not only recombinations are enhanced but also the uniform field approximation equation (1) is no longer valid.

Moreover, the negligible impact of geminate recombination on the current characteristic in bulk heterojunction featuring similar electrons and holes mobilities has already been observed in previous experimental studies, such as Ref. 12, for instance. In this work, the linear dependency of the short circuit current density j_{sc} versus incident light power has been identified as a signature of negligible bimolecular recombination. Our simulations, not reported here, confirm that when geminate recombination $(1-P) \times R$ is negligible compared to generation $P \times G$, j_{sc} is indeed a linear function of the incident light power. However, as pointed out in Ref. 19, this criterion may not be very accurate when the j_{sc} versus incident light curves appear "almost" linear.

Equation (2) can be analytically solved, leading to

$$p(x) = B + C \exp\left(\frac{e E x}{kT}\right) + \frac{P(E)G x}{\mu_p E}, \qquad (4)$$

where B and C are two integration constants. These constants can be determined by applying the standard boundary conditions for metal semiconductor contacts.[18] As shown in Fig. 2(a), the carrier concentration obtained using analytical equations (4) and (5) have been found in very good agreement with numerical results. Using a similar expression for

electrons, the total current density, which is the sum of the electron and hole current densities, reads

$$j(E) = j_{dark}(E) + j_{illu}(E), \qquad (5)$$

where

$$j_{illu}(E) = e\, P(E) G\, L \left[\frac{1}{\tanh\left(\dfrac{e E L}{2 kT}\right)} - \frac{2 kT}{e E L} \right], \qquad (6)$$

j_{dark} is the current in the absence of light, also derived in Refs. 11 and 20. j_{illu} is the photo generated current, typically higher than the dark current in reverse conditions, except around the open circuit voltage V_{OC}.

It is worth noticing that Eq. (6) includes and improves the result of Ref. 12. Indeed, in the latter work, neglecting the drift and diffusion of carriers, the current was simply modeled by the product $\pm P(E) \times G$. As shown in Figure 2(b), this approximation is qualitatively correct when $|E L/k T| \gg 1$, which is not the case around the open circuit voltage, where the diffusion of carriers has to be taken into account.

In order to simulate the impact of light on organic photodiodes, it is well known that the propagation of light inside the active layer has to be taken into account. This is typically achieved using the transfer matrix method,[7] considering an incident light beam perpendicular to the surface of the photodiode. To carry out these simulations, refractive indexes of each layers of the photodiode have been taken from Refs. 21 and 22.

Using this formalism, after integration over the illumination spectrum AM 1.5, the number of absorbed photons can be calculated at each point in the active layer, leading to a bounded electron-hole pairs' generation rate $G_{opt}(x)$. This effect has been included in our previous approach by replacing the constant generation rate G by the averaged electron-hole bounded pairs generation rate in the active layer, given by

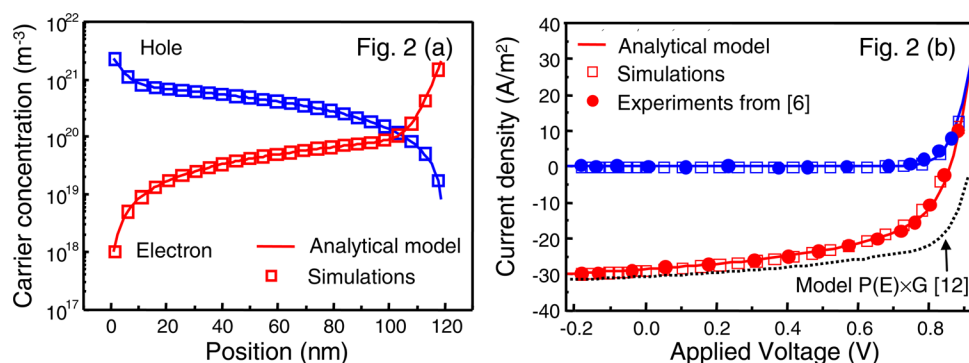$$G = \frac{1}{L} \int_0^L G_{opt}(x)\, dx. \qquad (7)$$

FIG. 2. (Color online) Comparison between drift and diffusion simulations (symbols) and analytical model (line): (a) electron and hole concentrations within the active layer; (b) I-V characteristics in dark and illuminated conditions. Experiments taken from Ref. 6 (circle symbols) are also shown for comparison. The same parameters (listed in Figure 1(b)) have been used for both simulations and model.

In the uniform generation rate case, the total current density equations (14)–(16) have been found in very good agreement with numerical simulations, as shown in Fig. 2(b). It has also been compared with experimental results taken from Ref. 6, as shown also in Fig. 2(b). The parameters used in our analytical model are the same as those used in Ref. 6 in their numerical simulations, and are listed in the figure caption. Solar cell fill factor and efficiency can be easily calculated from Eqs. (5) and (6). Using the parameter used in Figure 3, the fill factor has been estimated to be 55% and the power efficiency to be 2.5%. These values are in good agreement with results reported in the literature.[6,9]

Finally, to evaluate the validity of the model when optical interference plays a significant role, an analytical simulation of the short circuit current versus the active layer thickness has been performed and compared with numerical simulations and experiments from Ref. 8 as shown in Fig. 3. The diode considered in this simulation was the same as in Ref. 8: the device is a sandwich of 60 nm of ITO, 50 nm of Pedot Pss (considered as the injecting layer in the simulation), a layer of P3hT-Pcbm, and 30 nm of aluminum deposited in this order on a glass substrate. Again, all curves have been found in good agreement.

Note that our approach, based on the approximation of negligible geminate bimolecular recombination and uniform electric field, is valid only in organic solar cells featuring an active layer thinner than 250 nm. For thicker active layers,

simulations, not shown here, indicate that the difference between model and simulations would exceed 10%. Indeed, for thicker cells, the electric field profile is no longer uniform. In this later case, the Poisson equation has to be solved self-consistently with transport equations. However, due to their lower electric field, thicker organic cells features a lower power efficiency and are thus not of practical interest.

In summary, a simple and physically based analytical model has been proposed to capture the dark and photogenerated I-V characteristics of organic solar cell and photodiode, accounting for charge dissociation via the Onsager-Braun geminate recombination theory and optical propagation. Model has been found in very good agreements with both experiments and numerical simulations. These results emphasis the critical impact in organic materials of the electron-hole pair dissociation mechanisms on photosensitive device performances.
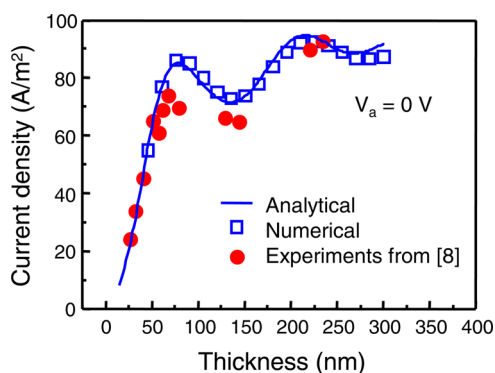

FIG. 3. (Color online) Short circuit current versus active layer thicknesses: comparison between experiments (Ref. 8) (open square symbols), numerical (filled square symbols), and analytical (lines) models. Parameters for these simulations are the same than the one used in Ref. 8, i.e., $\Delta\Phi_1 = 0.2$ eV, $\Delta\Phi_2 = -0.5$ eV, $L = 120$ nm, $\mu_p = 3 \times 10^{-4}$ cm^2 V^{-1} s^{-1}, $\mu_n = 2.5 \times 10^{-3}$ cm^2 V^{-1}, G corresponding to 1 sun, $k_f = 10^5$ s^{-1}, Eg = 1.6 eV, $\varepsilon_r = 3$. Device dimensions are $t_{ITO} = 125$ nm, $t_{Al} = 75$ nm, $t_{PEDOT} = 50$ nm. Only the electron-hole pair binding energy, which was not specified in Ref. 8, has been taken as an extract equal to $E_b = 0.329$ eV.

[1]Y. Yang and F. Wudl, Adv. Mater. **21**, 1401 (2009).
[2]D. V. Talapin, J. S. Lee, M. V. Kovalenko, and E. V. Shevchenko, Chem. Rev. **110**, 389 (2010).
[3]P. Peumans, A. Yakimov, and S. R. Forrest, J. Appl. Phys. **93**, 3693 (2003).
[4]G. Namkoong, P. Boland, K. Lee, and J. Dean, J. Appl. Phys. **107**, 124515 (2010).
[5]J. A. Barker, C. M. Ramsdale, and N. C. Greenham, Phys. Rev. B **67**, 075205 (2003).
[6]L. J. Koster, E. C. Smits, V. D. Mihailetchi, and P. W. Blom, Phys. Rev. B **72**, 085205 (2005).
[7]D. W. Sievers, V. Shrotriya, and Y. Yang, J. Appl. Phys. **100**, 114509 (2006).
[8]R. Häusermann, E. Knapp, M. Moos, N. A. Reinke, T. Flatz, and B. Ruhstaller, J. Appl. Phys. **106**, 104507 (2009).
[9]T. J. K. Brenner, I. Hwang, N. C. Greenham, and C. R. McNeill, J. Appl. Phys. **107**, 114501 (2010).
[10]P. Schilinsky, C. Waldauf, J. Hauch, and C. J. Brabec, J. Appl. Phys. **95**, 2816 (2004).
[11]P. Kumar, S. C. Jain, V. Kumar, S. Charand, and R. P. Tandon, J. Appl. Phys. **105**, 104507 (2009).
[12]R. A. Marsh, C. R. McNeill, A. Abrusci, A. R. Campbell, and R. H. Friend, Nano Lett. **8**, 1393 (2008).
[13]L. Onsager, J. Phys. Chem. **2**, 599 (1934).
[14]L. Onsager, Phys. Rev. **54**, 554 (1938).
[15]C. L. Braun, J. Chem. Phys. **80**, 4157 (1984).
[16]P. Langevin, Ann. Chim. Phys. **28**, 433 (1903).
[17]M. M. Mandoc, W. Veurman, L. J. Koster, B. de Boer, and P. W. M. Blom, Adv. Funct. Mater. **17**, 2167 (2007).
[18]S. M. Sze, *Physics of Semiconductors*, 2nd ed. (John Wiley & Sons, New York, 1981).
[19]K. Maturova, S. S. van Bavel, M. M. Wienk, R. A. Janssen, and M. Kemerink, Nano Lett. **9**, 3032 (2009).
[20]S. Altazin, R. Clerc, R. Gwoziecki, D. Boudinet, J. M. Verilhac, R. Coppard, G. Ghibaudo, G. Pananakakis, and C. Serbutoviez, Tech. Dig. - Int. Electron Devices Meet. **2009**, 387.
[21]H. Hoppe, N. S. Sariciftci, and D. Meissner, Mol. Cryst. Liq. Cryst. **385**, 233 (2002).
[22]F. Monestier, J. J. Simon, P. Torchio, L. Escoubas, B. Ratier, W. Hojeij, B. Lucas, A. Moliton, M. Cathelinaud, C. Defranoux, and F. Flory, Appl. Opt. **47**, C251 (2008).